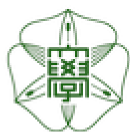

HOKKAIDO UNIVERSITY

Title	Thermopower Modulation Analyses of High-Mobility Transparent Amorphous Oxide Semiconductor Thin-Film Transistors
Author(s)	Yang, Hui; Zhang, Yuqiao; Matsuo, Yasutaka; Magari, Yusaku; Ohta, Hiromichi
Citation	ACS Applied Electronic Materials, 4(10), 5081-5086 https://doi.org/10.1021/acsaelm.2c01210
Issue Date	2022-10-25
Doc URL	http://hdl.handle.net/2115/90660
Rights	This document is the Accepted Manuscript version of a Published Work that appeared in final form in [JournalTitle], copyright © American Chemical Society after peer review and technical editing by the publisher. To access the final edited and published work see https://pubs.acs.org/articlesonrequest/AOR-AKPAHP7A29ADCR9JGZNE
Type	article (author version)
Additional Information	There are other files related to this item in HUSCAP. Check the above URL.
File Information	Revised manuscript.pdf

Instructions for use

Hokkaido University Collection of Scholarly and Academic Papers : HUSCAP

Thermopower Modulation Analyses of High-mobility Transparent Amorphous Oxide Semiconductor Thin-Film Transistors

Hui Yang[1,2,*], Yuqiao Zhang[3,4], Yasutaka Matsuo[1], Yusaku Magari[1,5], and Hiromichi Ohta[1,*]

[1]*Research Institute for Electronic Science, Hokkaido University, N20W10, Kita, Sapporo 001-0020, Japan*

[2]*Institute of Optoelectronic Technology, Beijing Jiaotong University, Beijing 100044, China*

[3]*Institute of Quantum and Sustainable Technology, Jiangsu University, Zhenjiang 212013, China*

[4]*Foshan (Southern China) Institute for New Materials, Foshan 528200, China*

[5]*Graduate School of Natural Science and Technology, Shimane University, Matsue, Shimane, 690-8504, Japan*

*Email: 19118044@bjtu.edu.cn, hiromichi.ohta@es.hokudai.ac.jp

KEYWORDS: $InSnZnO_x$, transparent amorphous oxide semiconductor, thermopower modulation, effective mass, carrier relaxation time

ABSTRACT: Transparent amorphous oxide semiconductor $InSnZnO_x$ (ITZO)-based thin-film transistors (TFTs) exhibit a high field effect mobility (μ_{FE}). Although ITZO-TFTs have attracted increasing attention as a next-generation backplane of flat panel displays, the origin of the high μ_{FE} remains unclear due to the lack of systematic quantitative analyses using thermopower (S) as the measure. Here, we show that the high μ_{FE} originates from an extremely light carrier effective mass (m^*) and a long carrier relaxation time (τ). The S measurements of several ITZO films with different carrier concentrations clarified that m^* of ITZO films is ~0.11 m_0, which is ~70% of that of a commercial oxide semiconductor, amorphous $InGaZnO_4$ (~0.16 m_0). We then fabricated bottom-gate-top-contact ITZO-TFTs displaying excellent transistor characteristics (μ_{FE} ~58 cm^2 V^{-1} s^{-1}) using amorphous AlO_x as the gate insulator and demonstrated that the effective thickness increases with the gate voltage. This suggests that the bulk predominantly contributes to the drain current, which results in τ as long as ~3.6 fs, which is quadruple that of amorphous $InGaZnO_4$-TFTs (~0.9 fs). The present results are useful to further improve the mobility of ITZO-TFTs.

INTRODUCTION

Transparent amorphous oxide semiconductor (TAOS)-based thin-film transistors (TFTs) exhibit a field-effect mobility (μ_{FE} ~10 cm^2 V^{-1} s^{-1}) one or two orders of magnitude higher than previously used a-Si TFTs (μ_{FE} ~0.5 cm^2 V^{-1} s^{-1})[1, 2]. Consequently, TAOS-TFTs are applied as the backplane of active-matrix flat-panel displays. Amorphous

$InGaZnO_4$ (IGZO hereafter)-based TFTs[3] have been commercially available since 2012[2]. Although they are widely used, the increased demand for high-resolution and high-definition displays necessitates TAOS-TFTs that exhibits higher μ_{FE} for pixel-driving circuits. Recently, amorphous $InSnZnO_x$ (ITZO hereafter)-based TFTs have attracted attention as next-generation TAOS-TFTs because they display a much higher μ_{FE} than that of IGZO-TFTs.

Numerous studies have reported that ITZO-TFTs possess high μ_{FE} values.[4-10] In 2021, Shiah *et al.*[6] found an ITZO-TFT with an extremely high μ_{FE} of 70 $cm^2 V^{-1} s^{-1}$, demonstrating the potential of these TFTs. However, the origin of their high μ_{FE} has yet to be clarified. Generally, the carrier effective mass (m^*) of the channel layer is an important parameter because m^* reflects the overlap integral of the adjacent *n*s orbitals, which comprise the conduction band bottom. m^* is inversely proportional to the mobility ($\mu = e \cdot \tau \cdot m^{*-1}$, where e and τ are the electron charge and the carrier relaxation time, respectively).

Some studies have investigated m^* of IZTO films.[11-13] In 2009, Buchholz *et al.*[12] reported that the m^* of ITZO films fabricated via pulsed laser deposition (PLD) decreased from 0.35 m_0 to 0.22 m_0 as the oxygen pressure during film deposition increased. Since m^* is a characteristic number, this decrease in m^* indicates that the chemical composition of ITZO films depends on the oxygen pressure. In 2013, Noh *et al.*[13] theoretically calculated the m^* of ITZO and found that m^* of ITZO is in the range of 0.22−0.28 m_0. In 2020, So *et al.*[11] reported that m^* of the ITZO films decreased from 0.61 to 0.44 m_0 with increasing the oxygen gas flow rate during the film deposition.

However, since m^* of a-IGZO films is ~0.17 m_0 ($m^* = m_d^*/2$, the density of states effective mass, m_d^* ~0.34 m_0),[14-16] the high carrier mobility cannot be explained solely using the m^* scenario.

Another parameter is τ. It is feasible that τ in ITZO is much longer than that of a-IGZO-TFTs. Generally, phonons, defects, and boundaries scatter carriers. In the case of TAOS, the contribution of phonons and defects on τ can be neglected. Although the effect of grain boundaries can be neglected, the gate insulator/TAOS boundary of the TAOS-TFTs may contribute to carrier scattering. Therefore, the effective channel thickness (t_{eff}) of ITZO-TFTs should be a suitable measure to analyze μ_{FE}. To date, t_{eff} of ITZO-TFTs has yet to be clarified.

This study systematically investigates the origin of the high μ_{FE} in ITZO-TFTs. Firstly, we fabricated several ITZO films with various carrier concentrations and measured the thermopower (S) and volume carrier concentration ($n_{3\mathrm{D}}$). The S–log $n_{3\mathrm{D}}$ relationship is a suitable measure to estimate m^* of TAOS with a parabolic-shaped conduction band bottom. The film quality does not affect the S measurement because S clearly reflects the energy differential of the density of states at the Fermi energy ($[\partial \mathrm{DOS}(E)/\partial E]_{E = E_\mathrm{F}}$). We estimated m^* of ITZO films as ~0.11 m_0. This value is ~70% of that of commercially applied oxide semiconductors, a-IGZO (~0.16 m_0). τ can be estimated as $\tau = \mu_{\mathrm{FE}} \cdot m^* \cdot e^{-1}$ (~3.6 fs), which is much longer than that of a-IGZO-TFTs (~0.9 fs). Then we fabricated bottom-gate-top-contact ITZO-TFTs. When amorphous AlO_x is used, ITZO-TFTs display excellent transistor characteristics (μ_{FE} ~58 cm^2 V^{-1} s^{-1}). We measured S as a function of the sheet carrier concentration ($n_{2\mathrm{D}}$) by applying a V_g, called

the electric field thermopower modulation method (see experimental section). Additionally, we estimated t_{eff} of the ITZO channel as $t_{eff} = n_{2D}/n_{3D}$ at the same S. t_{eff} increases with the V_g. These results suggest that the bulk predominately contributes to the drain current and may reflect the longer τ. Thus, the small m^* (~0.11 m_0) and long τ (~3.6 fs) are responsible for the high μ_{FE} of ITZO-TFTs. The present results should further enhance the mobility of ITZO-TFTs.

EXPERIMENTAL SECTION

Fabrication of ITZO films: Amorphous ITZO films were fabricated on alkali-free glass substrates (EAGLE XG®, Corning®) by pulsed laser deposition (PLD) at room temperature using a KrF excimer laser (~1.5 J cm^{-2} $pulse^{-1}$, 10 Hz, 1800 pulses). The chemical composition of the ITZO ceramic target was In:Sn:Zn at a 1.1:0.1:1 molar ratio. Inductively Coupled Plasma Mass Spectrometry (ICP-MS) indicated that the resultant chemical composition of the ITZO films was In:Sn:Zn = 1.6:0.16:1. To adjust the carrier concentration, the oxygen pressure was varied between 1−10 Pa during the deposition at a deposition rate of ~0.3 nm s^{-1}. Afterwards, the ITZO films were annealed at several temperatures (100−350 °C) in air for 5 min.

Electron transport property measurements of the ITZO films: X-ray reflectivity (XRR, ATX-G, Rigaku) and subsequent least square simulations precisely measured the film thickness, relative density, and surface roughness of the resultant ITZO films. The dc four-probe method using a van der Pauw electrode configuration measured the electrical resistivity (ρ), carrier concentration (n), and Hall mobility (μ_{Hall}) of the ITZO

thin films. S was measured by a conventional steady-state method at room temperature using laboratory-made equipment.

Fabrication of ITZO-TFTs: Bottom-gate & top-contact type ITZO-TFTs were fabricated on alkali-free glass substrates (EAGLE XG®, Corning®). Firstly, a 106-nm-thick amorphous AlO_x film (gate insulator, dielectric permittivity $\varepsilon_r = 8$) was deposited on an ITO-coated EAGLE XG® substrate via an atomic layer deposition (ALD, R-200 Advanced, Picosun Oy) technique. The capacitance (C_i) of the AlO_x films was 67 nF cm^{-2}. Then an amorphous ITZO film was deposited by PLD through a stencil mask at room temperature. Deposition occurred at a constant oxygen pressure of 5 Pa. Then the multilayer film was annealed at 350 °C for 5 min in air. Finally, a 20-nm-thick Ti film was deposited by electron beam evaporation through a stencil mask as source & drain electrodes.

Transistor characteristics and electric field thermopower modulation: The transistor characteristics of ITZO-TFTs were measured by a semiconductor device analyzer (B1500A, Agilent) at room temperature. Thermopower modulation analyses of the resultant TFTs were performed at room temperature in air. We have demonstrated electric field thermopower modulation analyses of $SrTiO_3$-TFTs[17, 18], $InGaZnO_4$-TFTs[19], $BaSnO_3$-TFTs[20-22], SnO_2-TFTs[23, 24], and GaN-TFTs[25] thus far.

RESULTS AND DISCUSSION

First, we fabricated several ITZO films with different n_{3D} values. n_{3D} was varied by controlling the oxygen pressure during film deposition. Then we measured the

thickness, relative density, and surface roughness. Next, we evaluated the Seebeck effect and Hall effect of the resultant ITZO films at room temperature. **Figure 1a** plots Hall mobility (μ_{Hall}) of the ITZO films as a function of n_{3D} at room temperature. μ_{Hall} gradually increases as n_{3D} increases. This trend is similar to that for a-IGZO films. The overall μ_{Hall} values are higher than those of a-IGZO (~10 cm^2 V^{-1} s^{-1}), which is consistent with the higher μ_{FE} of ITZO-TFT.

Figure 1b plots S of the ITZO films as a function of n_{3D} at room temperature. Consistent with ITZO being an n-type semiconductor, the S-values are all negative. The absolute value of S (|S|) gradually decreases with n_{3D}. We extracted m^* using the relationship between n_{3D} and S, which is described by equations (1) – (3).[26]

$$n_{3D} = 4\pi \left(\frac{2 \cdot m_d^* \cdot k_B \cdot T}{h^2}\right)^{1.5} F_r(\xi) \tag{1}$$

$$F_r(\xi) = \int_0^\infty \frac{x^r}{1+e^{x-\xi}} dx \tag{2}$$

$$S = -\frac{k_B}{e}\left(\frac{(r+2)F_{r+1}(\xi)}{(r+1)F_r(\xi)} - \xi\right) \tag{3}$$

where m_d^*, k_B, T, h, ξ, F_r, and r are the density of states effective mass (m_d^* = spin degeneracy × m^* = 2m^*), Boltzmann constant, absolute temperature, Planck constant, chemical potential, Fermi integral, and scattering parameter of the relaxation time (r = 0.5 denotes that optical phonon scattering is dominant), respectively. The observed S is well fitted with the calculated m^* = 0.11 m_0 line. Thus, m^* of the ITZO film is 0.11 m_0. This value is ~70% of that of a commercially applied oxide semiconductor, a-IGZO (~0.16 m_0, obtained from S measurements, data not shown). The small value of m^* indicates that the In 5s orbitals largely overlap in the ITZO films. Thus, we conclude that the lighter m^* of the ITZO film contributes to the high μ_{FE}.

Next, we fabricated ITZO-TFTs with various channel thicknesses (5 nm, 10 nm, 20 nm, 30 nm, 40 nm, 50 nm) and measured their transistor characteristics. The transfer characteristics and output characteristics were measured at room temperature. **Figure 2a** shows the typical transistor characteristics of 10-nm-thick a-ITZO TFTs. The intercept of the *x*-axis by fitting the square root of I_d ($I_d^{1/2}$) with respect to V_g with a straight line indicates that the threshold voltage (V_{th}) is −5.5 V.

a-ITZO TFTs exhibit excellent transistor characteristics (I_{ON}/I_{OFF} ~10^9, μ_{FE} ~58 $cm^2 V^{-1} s^{-1}$, subthreshold swing (*S.S.*) ~70 mV $decade^{-1}$). **Figure 2b** shows the output characteristics of a-ITZO TFTs. a-ITZO TFTs display clear pinch-off and current saturation characteristics at higher V_d, indicating that the TFT operation obeys the standard transistor theory. **Table S1** summarizes the transistor characteristics of ITZO-TFTs with various ITZO thicknesses. As the channel layer thickness increases from 5 to 50 nm, V_{th} monotonically decreases from −2.9 to −14.5 V. μ_{FE} initially increases but then decreases. In all TFTs, I_{ON}/I_{OFF} exceeds 10^8. In general, the 10-nm-thick TFT shows the best performance.

We then calculated τ as $\tau = \mu_{FE} \cdot m^* \cdot e^{-1}$. τ is ~3.6 fs, which is much longer than that of a-IGZO-TFTs (~0.9 fs). This suggests that τ may also contribute to the higher μ_{FE}. This study focuses on t_{eff} of ITZO-TFTs. We measured S of the ITZO-TFT channels with L = 800 μm and W = 400 μm upon applying V_g (**Fig. 3a**). First, a constant V_g was applied to the TFT to accumulate electron carriers. Then a temperature difference ΔT was given between the source and drain electrodes by two Peltier devices. The generated

thermoelectromotive force ΔV was measured.

n_{2D} of the channel layer was modulated by changing V_g ($n_{2D} = C_i (V_g - V_{th})$). **Figure 3b** plots the electric field modulated S as a function of n_{2D} of ITZO TFTs with various channel layer thicknesses. Note that the bias stress stability of the TFTs was good (**Fig. S1**), and the data collection of S during V_g application was stable. $|S|$ monotonically decreases with n_{2D} when the channel is less than 10-nm thick. In contrast, it turns upward upon further increasing n_{2D} when the channel is greater than 10-nm thick. These observations clearly indicate that the bulk predominantly contributes to the observed S.

Finally, we extracted $t_{eff} = n_{2D}/n_{3D}$ by comparing n_{2D} (**Fig. 3b**) with n_{3D} (**Fig. 1b**) at the same $|S|$. **Figure 4a** plots t_{eff} as a function of n_{2D}. In all cases, t_{eff} gradually increases with V_g. Interestingly, t_{eff} increases beyond the ITZO thickness as n_{2D} increases. This trend is not able to explain using standard field effect theory; In general, t_{eff} becomes thin with increasing the electric field because the electric field strongly attracts carrier electrons to the semiconductor/gate insulator interface.

Here, we discuss the unusual behavior of the electric field thermopower modulation in ITZO-TFTs. **Figure 4b** shows the energy band diagram around the conduction band of ITZO-TFTs. Since the ITZO films are degenerate semiconductors, E_F is located above the conduction band minimum (CBM), and the CBM is parabolic. Applying a positive V_g causes the free electrons to accumulate around the interface between the insulator layer (AlO_x) and the channel layer (ITZO). The S-value of ITZO-TFTs depends on both the A layer (interface layer) and the B layer (bulk layer), which is expressed as[18]

$$S = \frac{S_A \sigma_{sA} + S_B \sigma_{sB}}{\sigma_{sA} + \sigma_{sB}} \quad (4)$$

where S_A is the thermopower of the A layer, S_B is the thermopower of the B layer, σ_{sA} is the sheet conductance of the A layer, and σ_{sB} is the sheet conductance of the B layer.

When the channel is less than 10-nm thick, the A layer dominates the S value of the ITZO-TFTs. As V_g increases, t_{eff} becomes thinner due to band bending of the CBM, and the free carrier concentration around the A layer increases. Hence, S monotonously decreases as n_{2D} increases. In contrast, when the channel is greater than 10-nm thick, the B layer dominates S. As V_g increases, most of the free carriers accumulate at the A layer. Consequently, the CBM bending region is limited to 10 nm, resulting in the depletion of the B layer. When n_{2D} is larger than the threshold value, S should further increase. These observations clearly indicate that the bulk layer predominantly contributes to the drain current when the transistor is on. Since the bulk layer is far from the insulator/channel interface, τ of ITZO-TFTs is much longer than that of a-IGZO-TFTs. From these results, we judge that the lighter m^* (~0.11 m_0) and the longer τ (~3.6 fs) are the origin of the high μ_{FE}. The present results should contribute to improving the mobility of ITZO-TFTs.

CONCLUSION

S modulations systematically clarified the origin of the high μ_{FE} of a-ITZO-TFTs. S measurements of several ITZO films with various carrier concentrations revealed that m^* of ITZO films is ~0.11 m_0, which is ~70% of that of a-IGZO films (~0.16 m_0). We then fabricated bottom-gate-top-contact ITZO-TFTs with excellent transistor characteristics (μ_{FE} ~58 cm^2 V^{-1} s^{-1}) using amorphous AlO_x as the gate insulator. t_{eff}

increases with the V_g. τ is as long as ~3.6 fs because the bulk predominantly contributes to the drain current. This value is twice that of a-IGZO-TFTs (~0.9 fs). The lighter m^* (~0.11 m_0) and longer τ (~3.6 fs) are the origin of the high μ_{FE} of ITZO-TFTs. These results should further improve the mobility of ITZO-TFTs.

ASSOCIATED CONTENT

Supporting Information is available free of charge via the Internet at https://pubs.acs.org/doi/10.1021/acsaelm.XXXXXXX.

The transistor characteristics of the ITZO-TFTs with various ITZO thickness; Transfer characteristics of the 10-nm-thick a-ITZO TFTs under bias stress.

AUTHOR INFORMATION

Corresponding Authors

Hui Yang − Research Institute for Electronic Science, Hokkaido University, N20W10, Kita, Sapporo 001-0020, Japan & Institute of Optoelectronic Technology, Beijing Jiaotong University, Beijing 100044, China

ORCiD: orcid.org/ 0000-0002-2287-2243

Email: 19118044@bjtu.edu.cn

Hiromichi Ohta − Research Institute for Electronic Science, Hokkaido University, N20W10, Kita, Sapporo 001-0020, Japan

ORCiD: orcid.org/0000-0001-7013-0343

Email: hiromichi.ohta@es.hokudai.ac.jp

Author

Yuqiao Zhang − Institute of Quantum and Sustainable Technology, Jiangsu University, Zhenjiang 212013, China

Foshan (Southern China) Institute for New Materials, Foshan 528200, China

ORCiD: orcid.org/0000-0001-7579-4923

Yasutaka Matsuo − Research Institute for Electronic Science, Hokkaido University, N20W10, Kita, Sapporo 001-0020, Japan

ORCiD: orcid.org/0000-0002-5071-0284

Yusaku Magari − Research Institute for Electronic Science, Hokkaido University, N20W10, Kita, Sapporo 001-0020, Japan & Graduate School of Natural Science and Technology, Shimane University, Matsue, Shimane, 690-8504, Japan

ORCiD: orcid.org/0000-0001-9655-4283

Author Contributions

H.Y., Y. Matsuo, and H.O. fabricated the samples and measured the transistor characteristics and thermopower. Y.Z. analyzed the thermopower. Y.M. analyzed the transistor characteristics. H.O. planned and supervised the project. All authors discussed

the results and commented on the manuscript.

Funding Sources

Hui Yang received scholarship from China Scholarship Council (202107090085). Yusaku Magari received funding from a Grant-in-Aid of the JSPS (22K14303). Hiromichi Ohta received funding from Grants-in-Aid of the JSPS (19H05788, 22H00253). Yuqiao Zhang received funding from the Start-Up Fund of Jiangsu University (5501310015), Guangdong Basic and Applied Basic Research Foundation (2021A1515110881), and the Youth fund of Foshan (Southern China) Institute for New Materials (2021AYF25009).

Notes

The authors declare no competing interest.

ACKNOWLEDGEMENTS

This research was supported by a Grant-in-Aid for Innovative Areas (19H05791) from the Japan Society for the Promotion of Science (JSPS). Hui Yang is supported by CSC (202107090085). Y.Z. is supported by Guangdong Basic and Applied Basic Research Foundation (2021A1515110881). Y.M. is supported by a Grant-in-Aid for Young Scientists (22K14303) from JSPS. H.O. is supported by a Grant-in-Aid for Scientific Research A (22H00253) from JSPS. The authors thank Nozomi Takeda for the ICP-MS

measurements. Part of this work was supported by "Advanced Research Infrastructure for Materials and Nanotechnology in Japan (ARIM)" of the Ministry of Education, Culture, Sports, Science and Technology (MEXT). A part of this work was supported by the Network Joint Research Center for Materials and Devices.

REFERENCES

(1) Hosono, H. How we made the IGZO transistor. *Nat. Electron.* **2018,** 1, 428-428.

(2) Amorphous oxide semiconductors: IGZO and related materials for display and memory. Hosono, H.; Kumomi, H., Eds. Wiley: Hoboken, NJ, 2022.

(3) Nomura, K.; Ohta, H.; Takagi, A.; Kamiya, T.; Hirano, M.; Hosono, H. Room-temperature Fabrication of Transparent Flexible Thin-film Transistors using Amorphous Oxide Semiconductors. *Nature* **2004,** 432, 488-492.

(4) Song, J. H.; Kim, K. S.; Mo, Y. G.; Choi, R.; Jeong, J. K. Achieving High Field-Effect Mobility Exceeding 50 cm^2/Vs in In-Zn-Sn-O Thin-Film Transistors. *IEEE Electron Device Lett.* **2014,** 35, 853-855.

(5) Fuh, C.-S.; Liu, P.-T.; Fan, Y.-S.; Chang, C.-H.; Chang, C.-C. P-20: Performance Improvement for High Mobility Amorphous Indium-Zinc-Tin-Oxide Thin-Film Transistors. *SID Symposium Digest of Technical Papers* **2014,** 45, 1017-1020.

(6) Shiah, Y. S.; Sim, K.; Shi, Y.; Abe, K.; Ueda, S.; Sasase, M.; Kim, J.; Hosono, H. Mobility–stability trade-off in oxide thin-film transistors. *Nat. Electron.* **2021,** 4, 800-807.

(7) Zhong, W.; Li, G. Y.; Lan, L. F.; Li, B.; Chen, R. S. Effects of annealing temperature on properties of InSnZnO thin film transistors prepared by Co-sputtering. *RSC Adv.* **2018,** 8, 34817-34822.

(8) Choi, W. H.; Sheng, J.; Jeong, H. J.; Park, J. S.; Kim, M.; Jeon, W. Improved

performance and stability of In-Sn-Zn-O thin film transistor by introducing a meso-crystalline ZrO_2 high-*k* gate insulator. *J. Vac. Sci. Technol. A* **2019,** 37, 020924.

(9) Sheng, J. Z.; Han, J. H.; Choi, W. H.; Park, J.; Park, J. S. Performance and Stability Enhancement of In-Sn-Zn-O TFTs Using SiO_2 Gate Dielectrics Grown by Low Temperature Atomic Layer Deposition. *ACS Appl. Mater. Interfaces* **2017,** 9, 42928-42934.

(10) Wang, X. L.; Liang, L. Y.; Zhang, H. B.; Wu, H. J.; Li, W. F.; Ning, C.; Yuan, G. C.; Cao, H. T. Huge mobility enhancement of InSnZnO thin-film transistors via Al-induced microstructure regularization. *Appl. Phys. Lett.* **2021,** 119, 212102.

(11) So, H. S.; Jung, D. H.; Seok, H. J.; Kim, H. K.; Lee, H. Electrical and Optical Properties of Amorphous Indium-Zinc-Tin Oxide Thin Films: Oxygen Flow Dependence. *J. Kor. Phys. Soc.* **2020,** 76, 750-756.

(12) Buchholz, D. B.; Liu, J.; Marks, T. J.; Zhang, M.; Chang, R. Control and characterization of the structural, electrical, and optical properties of amorphous zinc-indium-tin oxide thin films. *ACS Appl. Mater. Interfaces* **2009,** 1, 2147-2153.

(13) Noh, J. Y.; Kim, H.; Nahm, H. H.; Kim, Y. S.; Kim, D. H.; Ahn, B. D.; Lim, J. H.; Kim, G. H.; Lee, J. H.; Song, J. Cation composition effects on electronic structures of In-Sn-Zn-O amorphous semiconductors. *J. Appl. Phys.* **2013,** 113, 183706.

(14) Takagi, A.; Nomura, K.; Ohta, H.; Yanagi, H.; Kamiya, T.; Hirano, M.; Hosono, H. Carrier transport and electronic structure in amorphous oxide semiconductor, a-$InGaZnO_4$. *Thin Solid Films* **2005,** 486, 38-41.

(15) Nomura, K.; Kamiya, T.; Ohta, H.; Uruga, T.; Hirano, M.; Hosono, H. Local coordination structure and electronic structure of the large electron mobility amorphous oxide semiconductor In-Ga-Zn-O: Experiment and ab initio calculations. *Phys. Rev. B*

2007, 75, 035212.

(16) Kamiya, T.; Nomura, K.; Hosono, H. Present status of amorphous In-Ga-Zn-O thin-film transistors. *Sci. Technol. Adv. Mater.* **2010,** 11, 044305.

(17) Ohta, H.; Masuoka, Y.; Asahi, R.; Kato, T.; Ikuhara, Y.; Nomura, K.; Hosono, H. Field-modulated thermopower in $SrTiO_3$-based field-effect transistors with amorphous $12CaO\cdot7Al_2O_3$ glass gate insulator. *Appl. Phys. Lett.* **2009,** 95, 113505.

(18) Ohta, H.; Mizuno, T.; Zheng, S.; Kato, T.; Ikuhara, Y.; Abe, K.; Kumomi, H.; Nomura, K.; Hosono, H. Unusually Large Enhancement of Thermopower in an Electric Field Induced Two-Dimensional Electron Gas. *Adv. Mater.* **2012,** 24, 740-744.

(19) Koide, H.; Nagao, Y.; Koumoto, K.; Takasaki, Y.; Umemura, T.; Kato, T.; Ikuhara, Y.; Ohta, H. Electric Field Modulation of Thermopower for Transparent Amorphous Oxide Thin Film Transistors. *Appl. Phys. Lett.* **2010,** 97, 182105.

(20) Sanchela, A.; Onozato, T.; Feng, B.; Ikuhara, Y.; Ohta, H. Thermopower modulation clarification of the intrinsic effective mass in transparent oxide semiconductor $BaSnO_3$. *Phys. Rev. Mater.* **2017,** 1, 5.

(21) Anup, V.; Sanchela; Mian; Wei; Hai, J.; Cho; Hiromichi; Ohta. Thermopower Modulation Clarification of the Operating Mechanism in Wide Bandgap $BaSnO_3$ -$SrSnO_3$ Solid-Solution Based Thin Film Transistors. *Small* **2019,** 15, 1805394.

(22) Kim, Y.; Kim, S.; Cho, H.; Kim, Y. M.; Ohta, H.; Char, K. Transport Properties of the $LaInO_3$/$BaSnO_3$ Interface Analyzed by Poisson-Schrödinger Equation. *Phys. Rev. Appl.* **2022,** 17, 014031.

(23) Liang, D. D.; Zhang, Y. Q.; Hai, J. C.; Ohta, H. Electric field thermopower modulation analyses of the operation mechanism of transparent amorphous SnO_2 thin-film transistor. *Appl. Phys. Lett.* **2020,** 116, 143503.

(24) Liang, D. D.; Chen, B. J.; Feng, B.; Ikuhara, Y.; Cho, H. J.; Ohta, H. Optimization of Two-Dimensional Channel Thickness in Nanometer-Thick SnO_2-Based Top-Gated Thin-Film Transistors Using Electric Field Thermopower Modulation: Implications for Flat-Panel Displays. *ACS Appl. Nano Mater.* **2020,** 3, 12427-12432.

(25) Ohta, H.; Kim, S. W.; Kaneki, S.; Yamamoto, A.; Hashizume, T. High Thermoelectric Power Factor of High-mobility 2D Electron Gas. *Adv. Sci.* **2018,** 5, 201700696.

(26) Vining; Cronin, B. A model for the high-temperature transport properties of heavily doped n-type silicon-germanium alloys. *J. Appl. Phys.* **1991,** 69, 331-341.

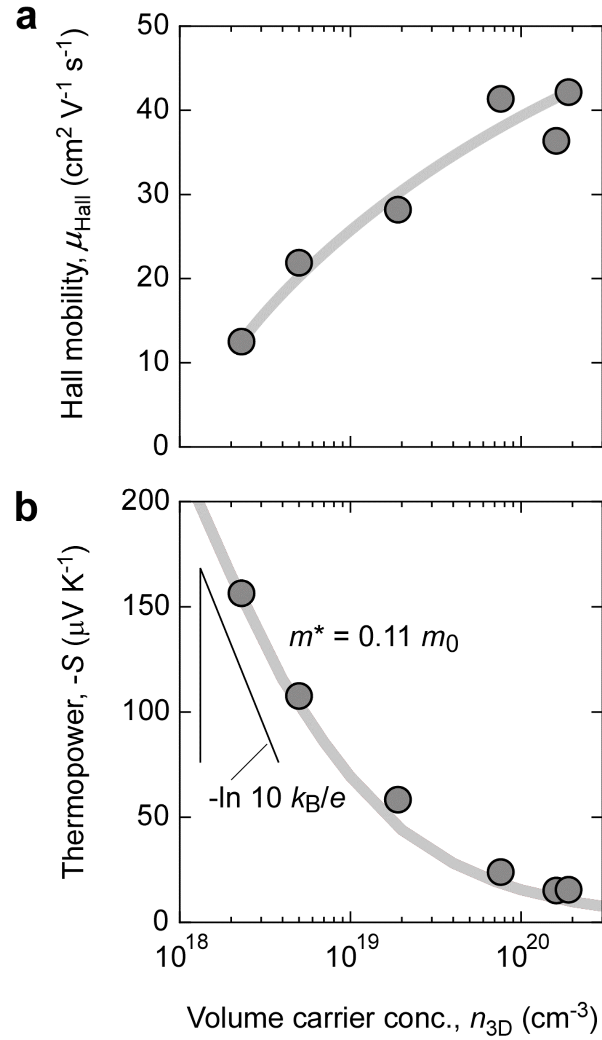

Figure 1. Electron transport properties of amorphous $InSnZnO_x$ (ITZO) films. (a) Hall mobility (μ_{Hall}) and (b) thermopower ($-S$) as a function of the volume carrier concentration (n_{3D}). μ_{Hall} gradually increases with n_{3D}. S-values are all negative, which is consistent with the fact that ITZO is an n-type semiconductor. m^* of ITZO films is 0.11 m_0.

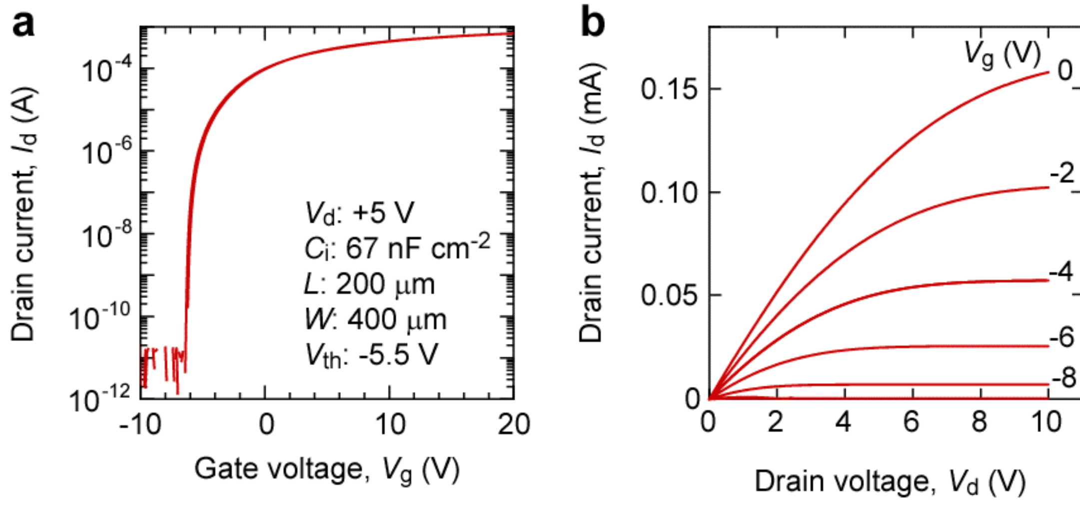

Figure 2. Typical transistor characteristics of 10-nm-thick a-ITZO-TFTs at room temperature. (a) Transfer characteristics and (b) output characteristics. Threshold voltage (V_{th}) is −5.5 V, subthreshold swing (*S.S.*) is ~70 mV decade^{-1}, and field effect mobility (μ_{FE}) is ~58 cm^2 V^{-1} s^{-1}.

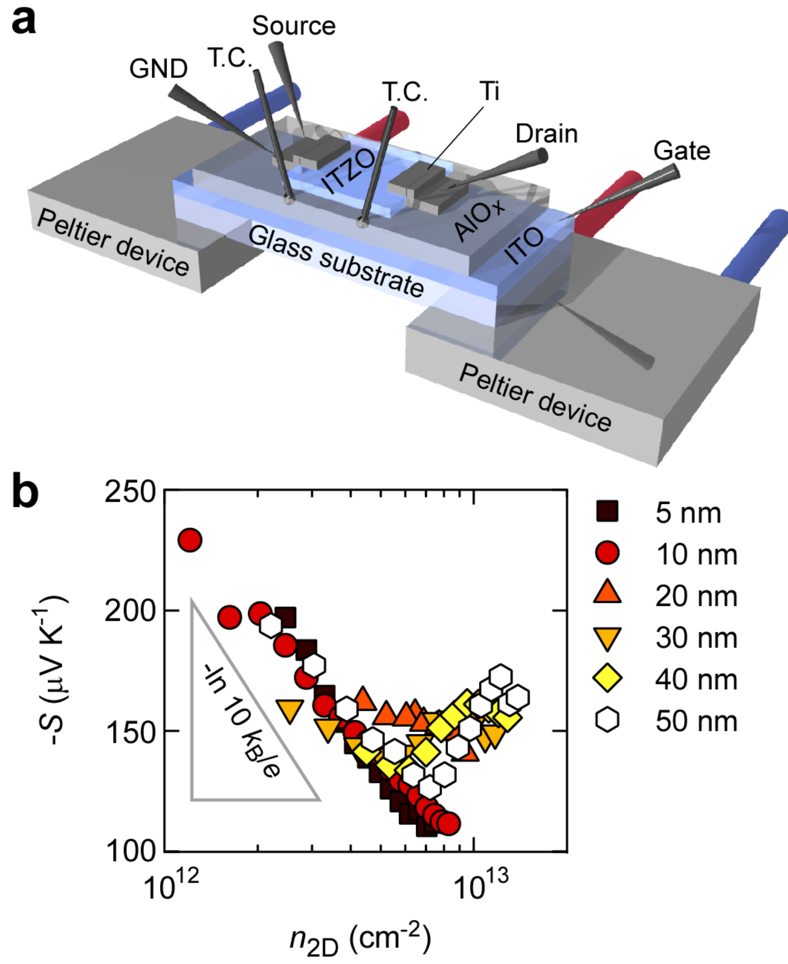

Figure 3. Electric field thermopower modulation measurement of the bottom-gate top contact a-ITZO-TFTs. (a) Schematic illustration of the measurement setup. Channel length (L) is 800 μm, and the channel width (W) is 400 μm. ITZO-TFT is placed on the gap (2 mm) between two Peltier devices, which are used to determine the temperature difference (ΔT). Two K-type thermocouples (T.C.) are located at both edges of the ITZO channel to measure the temperature between the edges of the ITZO channel. (b) S vs. sheet carrier concentration (n_{2D}) of the ITZO-TFTs. $|S|$ monotonically decreases with increasing n_{2D} when the channel is less than 10-nm thick, but it turns upward upon further increasing n_{2D} when the channel is greater than 10-nm thick.

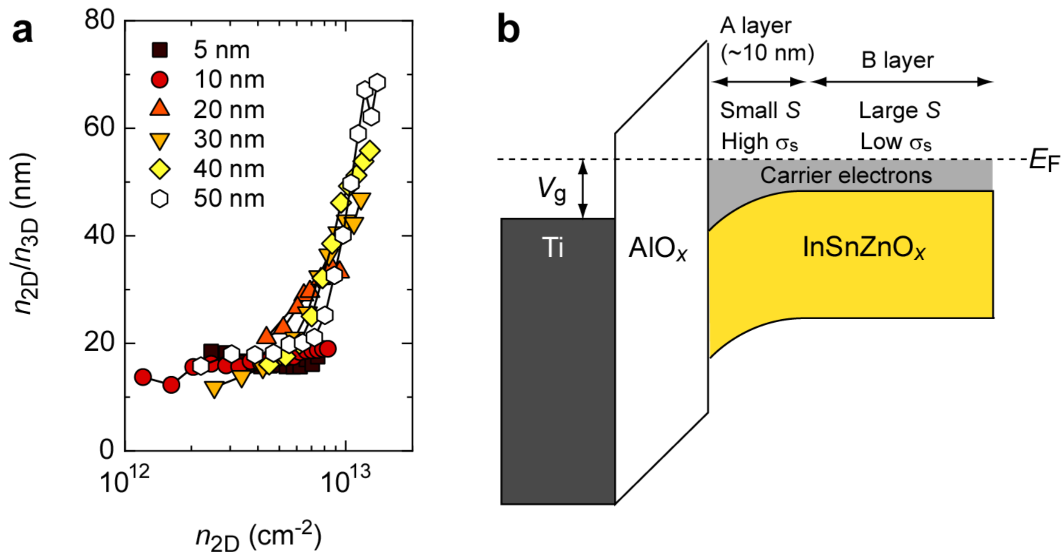

Figure 4. Operation mechanism of the ITZO-TFTs. (a) Change in t_{eff} (defined as n_{2D}/n_{3D}) as a function of n_{2D}. t_{eff} increases when n_{2D} exceeds 4×10^{12} cm^{-2}. (b) Schematic of the electric field carrier accumulation of a-ITZO-TFT. Both the A layer and the B layer contribute to the observable drain current and thermopower (S).